NMR Analysis of Covalent Intermediates in Thiamin Diphosphate Enzymes†

Kai Tittmann,*,‡ Ralph Golbik,‡ Kathrin Uhlemann,‡ Ludmila Khailova,§ Gunter Schneider,|| Mulchand Patel,⊥ Frank Jordan,# David M. Chipman,▽ Ronald G. Duggleby,○ and Gerhard Hübner#

Martin-Luther-Universität Halle-Wittenberg, Institut für Biochemie, Kurt-Mothes-Strasse 3, D-06099 Halle, Germany, A.N. Bakh Institute of Biochemistry, Russian Academy of Sciences, Moscow, Russia, Department of Medical Biochemistry and Biophysics, Karolinska Institutet, Stockholm, Sweden, Department of Biochemistry, School of Medicine and Biomedical Sciences, State University of New York at Buffalo, Buffalo, New York 14214, Department of Chemistry and the Program in Cellular and Molecular Biodynamics, Rutgers State University, Newark, New Jersey 07102, Department of Life Sciences, Ben-Gurion University of the Negev, Beer-Sheva, Israel, and Department of Biochemistry and Molecular Biology, The University of Queensland, Brisbane, Australia

Received March 21, 2003; Revised Manuscript Received May 9, 2003

ABSTRACT: Enzymic catalysis proceeds via intermediates formed in the course of substrate conversion. Here, we directly detect key intermediates in thiamin diphosphate (ThDP)-dependent enzymes during catalysis using ^{1}H NMR spectroscopy. The quantitative analysis of the relative intermediate concentrations allows the determination of the microscopic rate constants of individual catalytic steps. As demonstrated for pyruvate decarboxylase (PDC), this method, in combination with site-directed mutagenesis, enables the assignment of individual side chains to single steps in catalysis. In PDC, two independent proton relay systems and the stereochemical control of the enzymic environment account for proficient catalysis proceeding via intermediates at carbon 2 of the enzyme-bound cofactor. The application of this method to other ThDP-dependent enzymes provides insight into their specific chemical pathways.

Thiamin diphosphate (ThDP,[1] Figure 1A), the biologically active form of vitamin B_1, is an essential cofactor in biocatalysis being involved in numerous metabolic pathways, such as the oxidative and nonoxidative decarboxylation of α-keto acids (pyruvate dehydrogenase, pyruvate decarboxylase), the formation of amino acid precursors (acetohydroxyacid synthase), electron-transfer reactions (pyruvate oxidase, pyruvate:ferredoxin oxidoreductase), and ketol transfer between sugars (transketolase) (*1*, *2*). Recent studies on the mechanism of activation of enzyme-bound ThDP have revealed that the 4′-amino group of ThDP and a highly conserved interaction between a glutamate and the N1′ of the cofactor are integral components of a proton relay catalyzing a fast deprotonation of carbon 2 in ThDP (*3*). However, all subsequent steps in catalysis, which proceed via covalent adducts at C2 of the thiazolium ring of ThDP, have not been observed directly and in a time-resolved manner. The intermediate distribution was calculated either from carbon isotope effect studies (*4*, *5*) or from classical kinetics (*6*−*8*). Although the X-ray structures of many ThDP-dependent enzymes have been solved and provide insights into the spatial arrangement of the active sites (*9*−*14*), the molecular mechanism of single catalytic steps remains obscure or hypothetical. The rational design of active site variants with dramatically impaired catalytic constants and altered Michaelis constants provided evidence for the general catalytic involvement of individual side chains. However, no convincing conclusions could be drawn with respect to their specific contributions to single steps during catalysis.

In the studies presented here, we demonstrate that ^{1}H NMR is an ideal tool for analyzing the distribution of covalent intermediates in ThDP-dependent enzymes and their active site variants. Since this distribution correlates with the rates of individual steps of the interconversion of the intermediates, this new method enables the kinetic and mechanistic elucidation of enzymic catalysis at a molecular level.

MATERIALS AND METHODS

Chemical and Enzymatic Synthesis of Covalent ThDP Adducts. The presumed key intermediates in enzymic ThDP-catalysis, 2-lactyl-ThDP (LThDP), 2-(1-hydroxyethyl)-ThDP (HEThDP), 2-(1,2-dihydroxyethyl)-ThDP (DHEThDP), and 2-acetyl-ThDP (AcThDP) were chemically synthesized according to refs *15*−*18*. The purity and stability of all compounds were examined by ^{1}H NMR spectroscopy. The ^{1}H NMR chemical shifts of the C6′-H singlets of the aminopyrimidinium moiety (Figure 1A) can be used for the discrimination of all covalent ThDP adducts. From the

† This work was supported by the Deutsche Forschungsgemeinschaft and the Fonds der Chemischen Industrie, Australian Research Council Grant A09800834, U.S. Grant NIH-GM-50380, the Swedish Science Research Council, and a seed grant from the Research and Development Authority of Ben-Gurion University.

* To whom correspondence should be addressed. E-mail: kai@bc.biochemtech.uni-halle.de. Phone: ++49-345-5524887. Fax: ++49-345-5527011.

‡ Martin-Luther-Universität Halle-Wittenberg.

§ Russian Academy of Sciences.

|| Karolinska Institutet.

⊥ State University of New York at Buffalo.

Rutgers State University.

▽ Ben-Gurion University of the Negev.

○ The University of Queensland.

[1] Abbreviations: ThDP, thiamin diphosphate; HEThDP, 2-(1-hydroxyethyl)-ThDP; LThDP, 2-lactyl-ThDP; DHEThDP, 2-(1,2-dihydroxyethyl)-ThDP; AcThDP, 2-acetyl-ThDP; ALThDP, 2-[(1,2-dihydroxy-2-carboxy-1,2-dimethyl)-ethyl]-ThDP; *Zm*PDC, pyruvate decarboxylase from *Zymomonas mobilis*; *Sc*PDC, pyruvate decarboxylase from *Saccharomyces cereviseae*; AHAS, acetohydroxyacid synthase; POX, pyruvate oxidase; TK, transketolase.

10.1021/bi034465o CCC: $25.00
Published on Web 06/12/2003

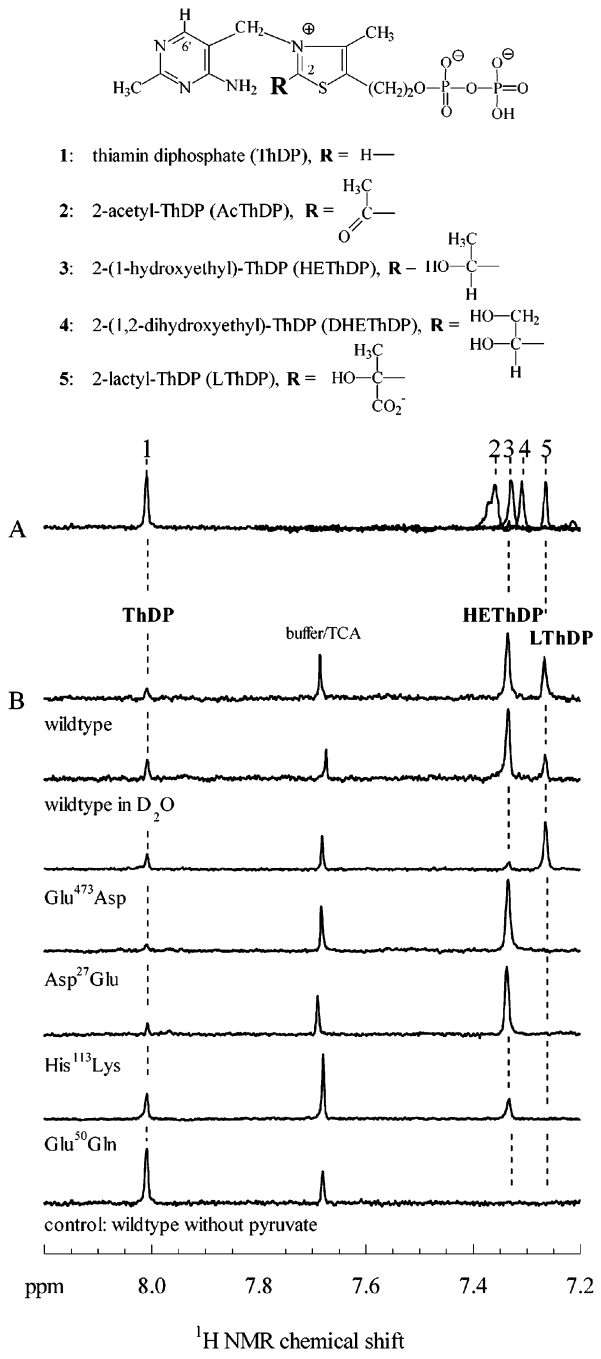

FIGURE 1: Covalent intermediates in ThDP-catalysis. (A) Chemical structures and C6′-H ^{1}H NMR fingerprint region of ThDP [**1**] and chemically synthesized intermediates occurring in nonoxidative [**3**,**5**] and oxidative enzymic decarboxylation of pyruvate [**2**,**3**,**5**] as well as in enzymic sugar transketolation [**4**] are shown. The two interfering signals of [**2**] represent the keto and hydrated form, respectively (*18*). Spectra were recorded at pH 0.75 and 25 °C. (B) Quantification of covalent intermediates in the nonoxidative decarboxylation of pyruvate by *Zm*PDC and selected enzyme variants under steady-state conditions and at substrate saturation (50 mM pyruvate). The intermediates were isolated by acid quench after a reaction time of 35 ms (wild-type) or 60 s (variants) and analyzed by ^{1}H NMR at pH 0.75 using the characteristic C6′-H chemical shifts. Their relative concentrations were determined from the relative integrals of the corresponding signals and used to calculate all microscopic rate constants of the catalytic cycle (Table 1).

integrated resolved peak areas of these signals, the intermediate distribution can be analyzed quantitatively. ^{1}H NMR chemical shifts δ ppm C6′-**H**: ThDP 8.01, LThDP 7.26, HEThDP 7.33, DHEThDP 7.31, and AcThDP 7.36, 7.37, 8.6 (AcThDP is in equilibrium with its hydrated form and an internal carbinolamine under these conditions) (*18*).

Since all chemical attempts to synthesize the covalent acetolactyl-ThDP (ALThDP, 2-[(1,2-dihydroxy-2-carboxy-1,2-dimethyl)-ethyl]-ThDP) intermediate de novo failed to date, we investigated the intermediate distribution of the Asp^{28}Ala variant of pyruvate decarboxylase from *Saccharomyces cerevisiae* (*Sc*PDC) that preferentially forms acetolactate instead of any other product (*19*). NMR-based investigation of the intermediate distribution of this variant at steady-state revealed the predominant presence of an acid stable covalent ThDP adduct (Figure 4A). The ^{1}H NMR spectrum of this intermediate is composed of all resonances typical of a covalent ThDP adduct with slightly altered chemical shifts and two additional methyl singlets. This is consistent with the structure of ALThDP.

Protein Expression and Purification. All proteins were purified to homogeneity using established protocols, and the enzymatic activity was determined according to refs *7* and *20*−*23*. In addition, enzyme-catalyzed substrate turnover and product formation were monitored directly by ^{1}H NMR spectroscopy.

Rapid Mixing Techniques and NMR Spectroscopy. In a typical experiment, 15 mg/mL pyruvate decarboxylase from *Zymomonas mobilis* (*Zm*PDC) in 50 mM sodium phosphate, pH 6.0 was mixed with 50 mM pyruvate (in the same buffer) at 30 °C using a RQF 3 chemical quenched-flow machine (Kintek Corp., Austin, Texas and Althouse). The reaction was stopped by the addition of 12.5% (w/v) TCA/1 M DCl (in D_2O). To ensure true steady-state conditions and substrate saturation of the enzyme, a set of experiments was conducted at varied reaction times (wild-type enzyme: 0−100 ms; enzyme variants: 0−300 s) and different pyruvate concentrations (0−100 mM). After separation of the precipitated protein by centrifugation, the ThDP intermediate distribution was analyzed by 1-D ^{1}H NMR spectroscopy using a Bruker Avance ARX 400 NMR spectrometer. For suppression of the water signal, a presaturation technique was used. A total of 32 000 data points were collected per scan over a spectral width of 12 ppm. Depending on the active site concentration of the protein, 1000−3000 scans were accumulated with an interscan delay of 2.5 s. Since the ratio of the integrated resolved peak areas of the intermediates is independent of the scan number, possible different relaxation properties of the intermediates do not effect the integral ratio. The baselines of the NMR spectra were corrected with a polynomial function. The peak integrals were determined with the program Xwinnmr. If peaks were not fully resolved, a software implemented deconvolution and integration routine was applied.

In a similiar way, the intermediate distributions of all other enzymes in this study were analyzed. The deprotonation rate constants at C2 of enzyme-bound ThDP were determined using a H/D exchange technique as described in ref *3*.

RESULTS AND DISCUSSION

On the basis of the excellent pioneering work of Holzer, Krampitz, Kluger, and Frey in the field of chemical synthesis and characterization of C2-ThDP adducts, the presumed key intermediates 2-lactyl-ThDP (LThDP), 2-(1-hydroxyethyl)-

Table 1: Microscopic Rate Constants of Elementary Catalytic Steps (Figure 2B) of *Zm*PDC Wild-Type (wt), *Zm*PDC Variants, and Pyruvamide-Activated *Sc*PDC Wild-Type

	k_{cat} (s^{-1})	k_{obs} (s^{-1})[a] H/D exchange at C2	k_2 (s^{-1})[b] C−C bonding	k_3 (s^{-1})[b] CO_2 release	k_4 (s^{-1})[b] acetaldehyde release
*Zm*PDC wt	**150 ± 5**	110 ± 19	2650 ± 210	**397 ± 20**	**265 ± 13**
*Zm*PDC wt (D_2O)	**100 ± 4**		685 ± 70	530 ± 45	**150 ± 14**
*Zm*PDC $Glu^{473}Asp$	**0.10 ± 0.004**	104 ± 20	**0.60 ± 0.08**	**0.13 ± 0.01**	1.2 ± 0.2
*Zm*PDC $Asp^{27}Glu$	**0.05 ± 0.002**	117 ± 13	>5	>5	**0.051 ± 0.002**
*Zm*PDC $His^{113}Lys$	**0.24 ± 0.03**	96 ± 24	>25	>25	**0.25 ± 0.03**
*Zm*PDC $Glu^{50}Gln$	**0.04 ± 0.003**	25 ± 7	**0.07 ± 0.01**	>7	**0.09 ± 0.01**
*Sc*PDC wt	**45 ± 2**	>600	294 ± 20	**105 ± 6**	**105 ± 6**

[a] H/D exchange rate constants of the enzyme-bound ThDP (k_{obs}, step 1 in Figure 2B) were determined according to ref *3* at 5 °C. [b] Rate constants of covalent pyruvate binding to ThDP (k_2), decarboxylation of LThDP (k_3), and acetaldehyde release from HEThDP (k_4) were calculated from the intermediate distribution (Figure 1B) and k_{cat} (eqs 2−7) measured at 30 °C in 50 mM sodium phosphate, pH 6.0. The steady-state intermediate distribution was corrected for the fraction of dissociated ThDP determined from the differences in activity in the presence and absence of excess ThDP (wt, $Glu^{473}Asp$, $Asp^{27}Glu$: <1%; $His^{113}Lys$, $Glu^{50}Gln$: ≈ 5%). Rate-limiting steps are indicated in bold type. Lower limits of the rate constants k_2 and k_3 reflect a limit of resolvability of the ^1H NMR spectra (signal-to-noise ratio = 3).

ThDP (HEThDP), 2-acetyl-ThDP (AcThDP), and 2-(1,2-dihydroxyethyl)-ThDP (DHEThDP) (Figure 1A) have been synthesized (*15*−*18*). None of these compounds undergoes decomposition below pH 1, and all of them can be discriminated unequivocally using ^1H NMR under these conditions. The ^1H NMR chemical shifts of the C6′-H singlets of the aminopyrimidinium moiety can be used as a fingerprint region for the discrimination of all C2-derived covalent ThDP adducts (Figure 1A). These properties allow the determination of the distribution of all covalent ThDP intermediates formed at steady-state in enzymic ThDP-catalysis by acid quench of the enzymic reaction and the subsequent simultaneous, quantitative, and direct detection of the isolated intermediates on the basis of differences in their ^1H NMR spectra. Since the distribution correlates with the rates of individual steps of their interconversion during catalysis, this new method enables the elucidation of enzymic catalysis at a detailed molecular level.

To test the feasibility of this NMR approach, both the bacterial pyruvate decarboxylase (PDC, EC 4.1.1.1) from *Z. mobilis* (*Zm*PDC) and the allosterically regulated enzyme from *S. cerevisiae* (*Sc*PDC) were investigated under steady-state conditions. These enzymes catalyze the nonoxidative decarboxylation of pyruvate yielding acetaldehyde and carbon dioxide. The minimal catalytic scheme comprises the reversible, noncovalent binding of the substrate (Michaelis complex, K_1), carbon−carbon bond formation between the C2 of ThDP and the carbonyl-carbon of pyruvate to yield enzyme-bound LThDP (k_2), the subsequent decarboxylation to the α-carbanion of HEThDP (k_3), and finally, the liberation of acetaldehyde (k_4). Although covalent binding of pyruvate to ThDP can be assumed to be reversible, the rate constant k_2, calculated from the intermediate distribution in steady-state, mainly reflects the forward reaction of this microscopic step because of the large forward commitment factor of LThDP decomposition ($k_{-2} \ll k_3$) (*5*).

$$\text{E-ThDP} + CH_3COCOO^- \overset{K_1}{\rightleftharpoons} \text{E-ThDP*}CH_3COCOO^- \xrightarrow{k_2} \text{E-LThDP}^- \xrightarrow[-CO_2]{k_3} \text{E-HEThDP}^- + H^+ \xrightarrow{k_4} \text{E-ThDP} + CH_3CHO \quad (1)$$

^1H NMR spectroscopic analysis of the covalent intermediates of wild-type *Zm*PDC, working with pyruvate at saturating concentrations in the steady-state, showed directly the existence of LThDP and HEThDP as intermediates and the appearance of ThDP (Figure 1B). In an enzymic reaction, all intermediates reach a constant level at steady-state characterized by equal rates of formation and decomposition. Therefore, based on the measured steady-state distribution of all intermediates and k_{cat}, the microscopic rate constants of the entire catalytic cycle (Table 1) can be calculated according to the following equations:

$$[\text{ThDP}]/[\text{LThDP}] = k_3/k_2 = a \quad (2)$$

$$[\text{ThDP}]/[\text{HEThDP}] = k_4/k_2 = b \quad (3)$$

$$k_{cat} = \frac{k_2k_3k_4}{k_2k_3 + k_2k_4 + k_3k_4} \quad (4)$$

$$k_2 = \frac{k_{cat}(a + b + ab)}{ab} \quad (5)$$

$$k_3 = \frac{k_{cat}(a + b + ab)}{b} \quad (6)$$

$$k_4 = \frac{k_{cat}(a + b + ab)}{a} \quad (7)$$

The resulting rate constants show that both decarboxylation ($k_3 = 397 \pm 20\ s^{-1}$) and acetaldehyde release ($k_4 = 265 \pm 13\ s^{-1}$) are partially rate-limiting and the formation of enzyme-bound LThDP to be very fast ($k_2 = 2650 \pm 210\ s^{-1}$). The steady-state intermediate distribution was also determined for the pyruvamide-activated *Sc*PDC (data not shown) resulting in comparable rate constants for both decarboxylation and acetaldehyde release (k_3, $k_4 = 105 \pm 6\ s^{-1}$) (Table 1). The rate constants for both *Zm*PDC as well as *Sc*PDC estimated from carbon isotope effect studies (*Zm*PDC: $k_3 \approx 300\ s^{-1}$, $k_4 \approx 200\ s^{-1}$; *Sc*PDC: $k_3 \approx 160\ s^{-1}$, $k_4 \approx 160\ s^{-1}$) (*4*, *5*) are in good agreement with our NMR results.

The method opens up the possibility for a detailed mechanistic elucidation of single steps of ThDP catalysis by using rationally designed enzyme variants. We determined the steady-state intermediate distribution and the H/D

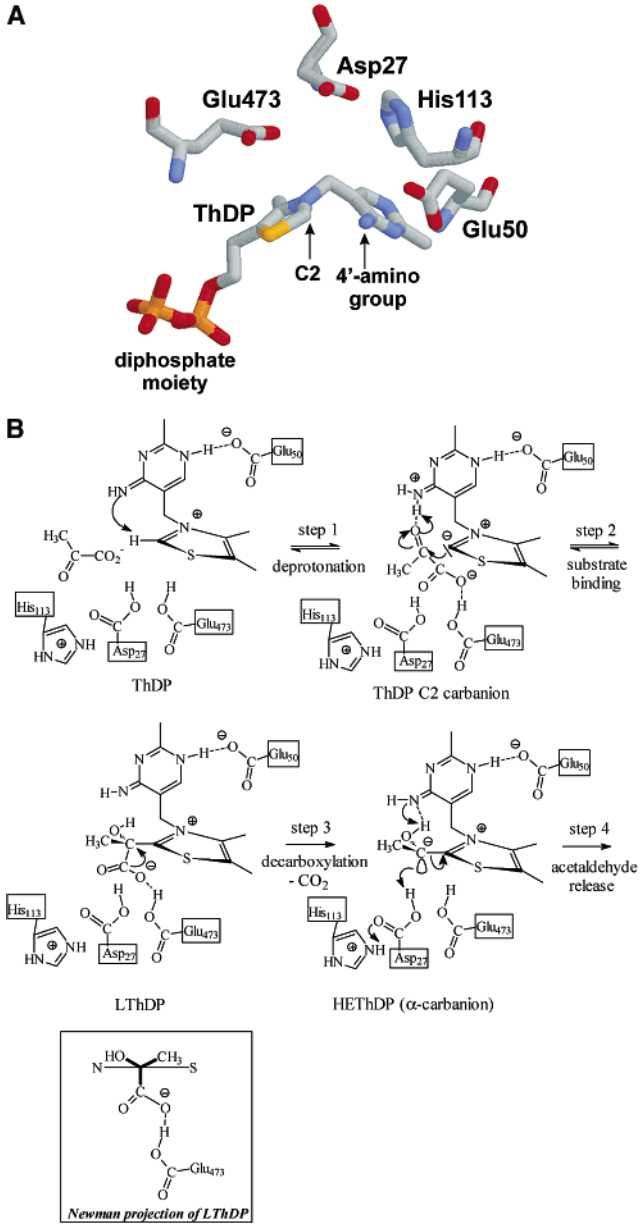

FIGURE 2: Active site of *Zm*PDC and suggested model of catalysis. (A) The crystal structure of active site residues of *Zm*PDC with the enzyme-bound cofactor ThDP in its typical V conformation is shown (*11*). (B) Proposed catalytic mechanism of PDC. The suggested roles of active site residues for the different steps of catalysis are consistent with the intermediate distribution during enzymic decarboxylation of pyruvate by PDC and its variants. This mechanism includes the action of two independent proton relay systems catalyzing the activation of ThDP (Glu^{50}-N1′-4′-NH_2, step 1), substrate binding (Glu^{50}-N1′-4′-NH_2, step 2), and acetaldehyde release (Glu^{50}-N1′-4′-NH_2 and His^{113}-Asp^{27}, step 4) as well as the stereochemical control of decarboxylation by glutamate 473 inducing a perpendicular orientation of the substrate carboxylate to the thiazolium ring of the enzyme-bound ThDP (Glu^{473}, steps 2 and 3), shown in the Newman projection.

exchange rate constant at C2 (ThDP) of various active site variants of *Zm*PDC (Figure 1B) displaying impaired overall activity. Variants of Glu^{473} (which is in a perpendicular orientation to the thiazolium moiety of ThDP), of Asp^{27} and His^{113} (which are in hydrogen bonding distance to each other in the active site cleft), and of Glu^{50} (which interacts with the N1′ of the enzyme-bound ThDP) were investigated (Figure 2A).

The mutation Glu^{473}Asp severely slows down carbon−carbon bond formation between the C2 of ThDP and the C_α of pyruvate as well as the decarboxylation of LThDP resulting in an accumulation of LThDP in the steady-state. In contrast, the rate constant of C2-H ionization is not affected by this mutation (Table 1). For the Asp^{27}Glu variant, only HEThDP can be detected under steady-state conditions suggesting that the product release from HEThDP is completely rate-limiting. A similiar deficiency in catalyzing acetaldehyde elimination from HEThDP is observed in the His^{113}Lys variant. Since His^{113} is in hydrogen bonding distance to Asp^{27}, this pair of residues apparently forms a functional dyad to assist acetaldehyde release. Perturbation of this proton relay system in either geometric or thermodynamic (ΔpK_a) terms disturbs the product elimination from HEThDP by several orders of magnitude (Table 1). Previous experiments suggested that the interaction between Glu^{50} and N1′ of the enzyme-bound ThDP acts as a chemical trigger for the reactivity of the 4′-amino group of the cofactor (*3*). The C2-H ionization rate constant in the Glu^{50}Gln variant is decreased in comparison to the wild-type enzyme, albeit to a lesser extent than found in homologous variants of other ThDP-dependent enzymes, and is not rate-limiting. The steady-state distribution of ThDP-derived intermediates in this enzyme variant consists of ThDP and HEThDP, demonstrating the involvement of the 4′-amino group in substrate binding as well as in the cleavage of HEThDP. In summary, effects are observed in C2-H ionization (Glu^{50}-Gln), covalent addition of pyruvate (Glu^{50}Gln, Glu^{473}Asp), decarboxylation of LThDP (Glu^{473}Asp), and acetaldehyde elimination from HEThDP (Glu^{50}Gln, Asp^{27}Glu, His^{113}Lys). Finally, primary isotope effects were determined for individual steps by comparing the relative intermediate distribution in H_2O and D_2O at steady-state. When catalysis is allowed to proceed in D_2O, the binding of pyruvate and product release, both requiring proton transfer steps, show primary isotope effects, whereas decarboxylation of LThDP is nearly unaffected (Table 1, Figure 1B).

On the basis of the steady-state intermediate distribution and the C2 (ThDP) deprotonation rate constants of the wild-type enzyme and the active site variants with defined deficiencies (Table 1), we propose a chemical mechanism of the catalytic cycle that is consistent with the obtained data (Figure 2B). The first microscopic step, the C2 deprotonation, is catalyzed by the 4′-imino group of ThDP since a perturbation of the proton relay between Glu^{50} and N1′ of ThDP as well as removing the 4′-amino group of the cofactor results in decreased deprotonation rates in PDC (*3*, *24*). In contrast, alterations of all other potential acid/base catalysts in the active site do not impair C2 anion formation (Table 1). The next step in catalysis, the carbon−carbon bond formation between the C2 carbanion of ThDP and the carbonyl carbon of the substrate, requires a protonation of the carbonyl oxygen of the substrate and its steric orientation. On one hand, the proton relay between Glu^{50}, N1′, and the 4′-amino group of ThDP as well as the Glu^{473}Asp mutation strongly influence the carbon−carbon bond formation. On the other hand, Glu^{473} is in a favorable position (Figure 2B) for an interaction with the carboxylate of LThDP. Therefore, we conclude that the proton relay protonates the carbonyl oxygen, whereas Glu^{473} plays an important role in the orientation of the substrate in the course of covalent substrate

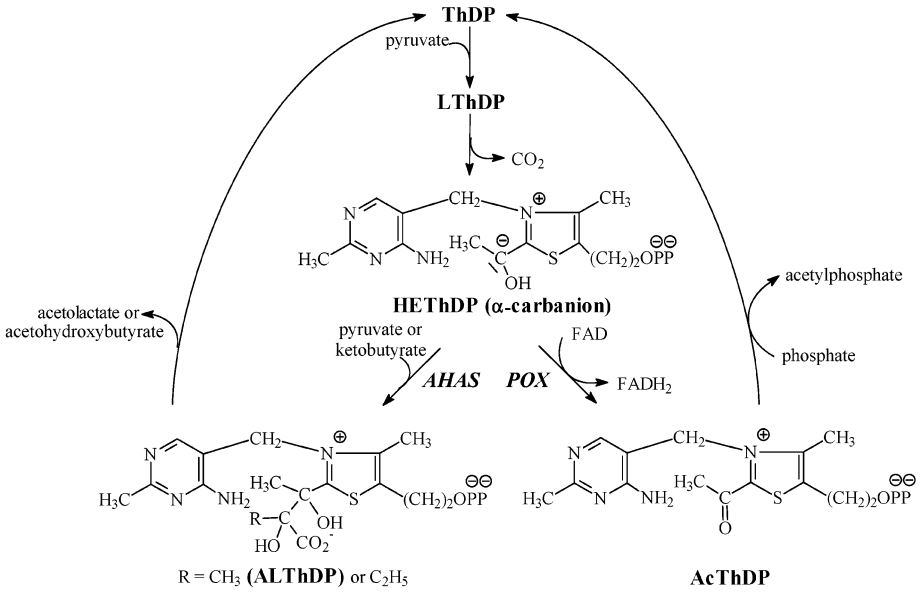

FIGURE 3: Key intermediates in the catalytic cycles of AHAS and POX.

binding and in the stereochemical control of the decarboxylation by causing a perpendicular orientation of the carboxylate of LThDP with respect to the thiazolium ring. This conformation leads to a maximum resonance stabilization of the built α-carbanion as already proposed as a least motion, maximum overlap mechanism for the nonenzymic system and in theoretical studies (*25*−*28*). The last step in catalysis, the elimination of acetaldehyde, comprises both the protonation of the α-carbanion and the deprotonation of the α-hydroxyl group of HEThDP. The His^{113}/Asp^{27} dyad is likely involved in the protonation of the α-carbanion since a mutation of either of those functional groups slows down acetaldehyde release. This suggested function of the dyad is further buttressed by the ability of Asp^{27} variants to catalyze acetolactate formation, a product formed by the electrophilic attack by a second pyruvate on the populated carbanion in this variant (*29*), hence clearly pointing to an accumulation of the α-carbanion/enamine of HEThDP in these variants and implying a perturbation of the protonation reaction. The ligation reaction is usually catalyzed by acetohydroxyacid synthase (AHAS), another ThDP-dependent enzyme (Figure 3). Strikingly, the His/Asp dyad is missing in this enzyme. A mutation of Glu^{50} drastically decreases the rate of acetaldehyde release and therefore favors the 4′-imino group of the cofactor as the only other remaining acid/base catalyst assisting acetaldehyde release as the promoter of deprotonation of the α-hydroxyl group of HEThDP.

To investigate whether this fingerprint NMR approach is suitable for the determination of the intermediate distribution in other ThDP-dependent enzymes that act on pyruvate, we applied this method to acetohydroxyacid synthase from *E. coli* (*Ec*AHAS II, EC 4.1.3.18), pyruvate oxidase from *Lactobacillus plantarum* (*Lp*POX, EC 1.2.3.3), and mammalian pyruvate dehydrogenase (PDH, EC 1.2.4.1). A detailed comparison of all microscopic steps in a series of ThDP-dependent enzymes, which catalyze different chemical reactions using the same cofactor and the same substrate, would reveal common chemical characteristics as well as unique features among this enzyme class. The first half reaction of catalysis of all these enzymes, culminating in the build-up of the α-carbanionic form of HEThDP, is identical to that of PDC (Figure 2B), but all subsequent steps are divergent.

AHAS catalyzes the covalent addition of a second pyruvate to the HEThDP intermediate yielding acetolactate (Figure 3). Apparently, the catalytic cycle of AHAS comprises an additional covalent ThDP adduct, which can be described as active acetolactate (ALThDP, see Materials and Methods). The most populated species in AHAS II catalysis using pyruvate as the only substrate is ThDP, whereas only small amounts of the intermediates LThDP, HEThDP, and ALThDP are detectable (Figure 4A). These observations concur with the detection of only ~0.01 HEThDP/mol enzyme using [^{14}C]-pyruvate (*30*). Consequently, the addition of pyruvate to the C2 of ThDP must be rate-limiting, while all other catalytic steps are comparatively fast (Table 2). AHAS II catalysis using α-ketobutyrate as an alternative second substrate (Figure 3) proceeds with a similar k_{cat} as the reaction with pyruvate despite the fact that α-ketobutyrate is preferred over pyruvate 60-fold (*31*). To understand this phenomenon, an intermediate analysis of AHAS II catalysis was performed in the presence of equimolar amounts of pyruvate and α-ketobutyrate (data not shown). The same rate constants for initial pyruvate binding and decarboxylation of LThDP were measured, whereas the binding of α-ketobutyrate and the release of the reaction product acetohydroxybutyrate are faster than the corresponding reactions with pyruvate as the second substrate (Table 2).

POX transfers two electrons from HEThDP to the adjacent FAD yielding AcThDP, which is cleaved phosphorolytically to acetyl phosphate and ThDP (Figure 3). If electron transfer between HEThDP and FAD is blocked by reducing the enzyme-bound FAD prior to or in the course of catalysis, all active sites in POX are occupied by HEThDP (Figure 4B). Furthermore, the accumulation of AcThDP in the absence of the substrate phosphate, which was indirectly inferred by earlier kinetic studies (*21*), could now be directly detected. In contrast, LThDP and a minor fraction of HEThDP are detectable at steady-state in the presence of phosphate (Figure 4B).

Pyruvate dehydrogenase (PDH, EC 1.2.4.1) complex is a multienzyme complex consisting of three components (E1,

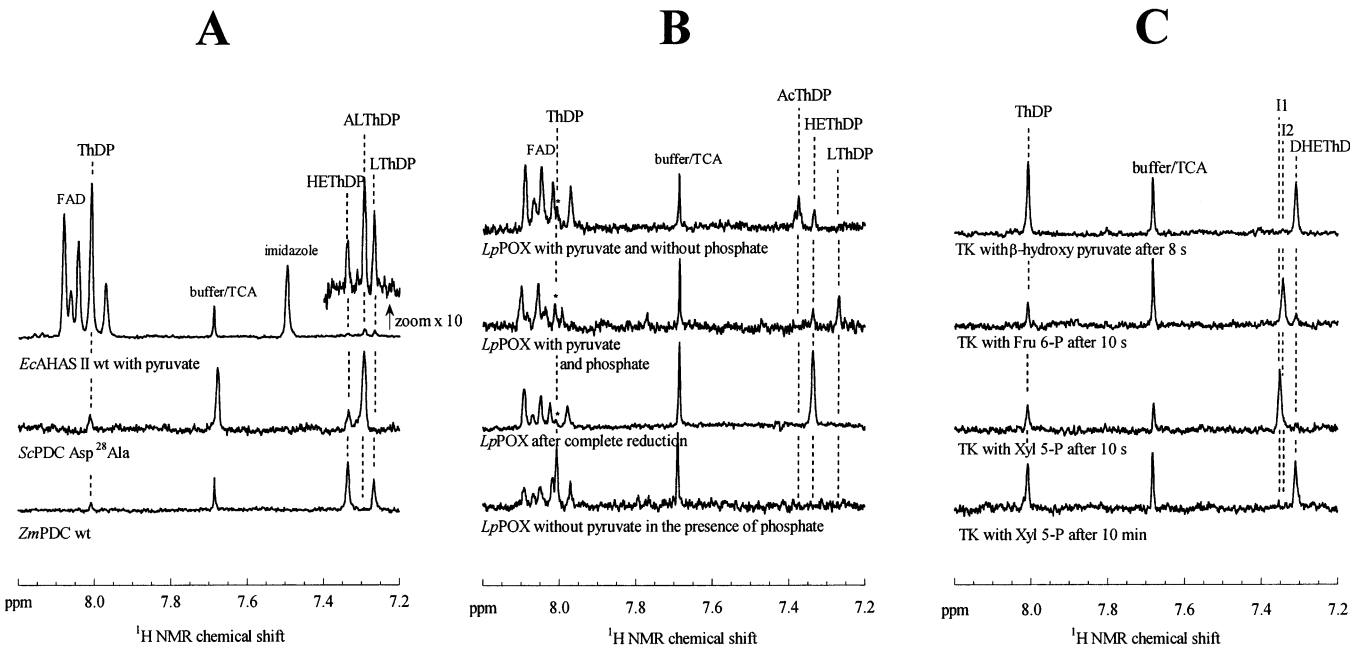

FIGURE 4: Detection of covalent intermediates in the superfamily of ThDP-dependent enzymes including acetohydroxyacid synthase (AHAS), pyruvate oxidase (POX), and transketolase (TK). (A) Covalent intermediates at steady-state and substrate saturation (50 mM pyruvate) of AHAS II (in 50 mM potassium phosphate, pH 7.6 at 37 °C) and of Asp[28]Ala PDC (in 50 mM potassium phosphate, pH 6.0 at 30 °C) from *S. cereviseae* that produces acetolactate exclusively (*19*) are shown. (B) Covalent intermediates at steady-state and substrate saturation (50 mM pyruvate, 200 mM phosphate) of POX in (a) the presence of pyruvate and phosphate (50 ms reaction time in 0.2 M potassium phosphate, pH 6.0 at 25 °C), (b) with pyruvate and in the absence of phosphate (100 s reaction time in 0.1 M MES/NaOH, pH 6.0 at 25 °C), and (c) after complete reduction of the enzyme-bound FAD (10 s reaction time in 0.2 M potassium phosphate, pH 6.0 at 25 °C) are shown. (C) Covalent intermediates during conversion of different donor substrates (0.25 mM *β*-hydroxy-pyruvate, 25 mM xylulose 5-phosphate and fructose 6-phosphate in 0.02 M sodium phosphate, pH 7.6 at 30 °C) by TK are shown. The intermediates I1 and I2 can be attributed to the 2-[2-(1,2,3,4,5-pentahydroxy)-pentyl]-ThDP and 2-[2-(1,2,3,4,5,6-hexahydroxy)-hexyl]-ThDP derivatives based on the chemical pathway.

Table 2: Microscopic Rate Constants of Elementary Catalytic Steps of AHAS II Wild Type in the Presence of Pyruvate (P + P, Product Acetolactate) or Pyruvate and α-Ketobutyrate (P + KB, Product Acetohydroxybutyrate) (Figure 3)[a]

	k_{cat} (s^{-1})	k_2 (s^{-1}) C−C bonding ThDP + pyruvate	k_3 (s^{-1}) CO_2 release	k_4 (s^{-1}) C−C bonding HEThDP + 2nd substrate	k_5 (s^{-1}) product release
AHAS II (P + P)	20 ± 0.2	**24 ± 4**	530 ± 70	1060 ± 175	176 ± 36
AHAS II (P + KB)	20 ± 0.2	**21 ± 4**	399 ± 54	>2000	>2000
*Sc*PDC Asp[28]Ala (P + P)	0.052 ± 0.001	>1	>1	0.36 ± 0.05	**0.073** ± 0.007

[a] Rate constants of covalent pyruvate binding to ThDP (k_2), decarboxylation of LThDP (k_3), covalent binding of the second substrate molecule (k_4), and product release (k_5) were calculated from the intermediate distribution (Figure 4A) and k_{cat}, determined at 37 °C in 50 mM potassium phosphate, pH 7.6 (AHAS) and in 50 mM potassium phosphate, pH 6.0 at 30 °C (PDC), respectively. The steady-state intermediate distribution was corrected for the fraction of dissociated ThDP determined from the differences in activity in the presence and absence of excess ThDP. Rate-limiting steps are indicated in bold type. Lower limits of the rate constants reflect a limit of resolvability of the ^{1}H NMR spectra (signal-to-noise ratio = 3).

E2, E3) catalyzing the oxidative decarboxylation of pyruvate with NAD^+ and coenzyme A as cosubstrates and yielding the essential metabolite acetyl-CoA. The ThDP-dependent E1 (decarboxylase) component binds and decarboxylates pyruvate resulting in the formation of the carbanion/enamine of HEThDP. We investigated the time-resolved distribution of ThDP, LThDP, and HEThDP for the mammalian E1 component as well as for the whole PDH complex under single-turnover conditions using pyruvate as the sole substrate.

$$\text{E-ThDP} + \text{CH}_3\text{COCOO}^- \overset{K_1}{\rightleftharpoons} \text{E-ThDP*CH}_3\text{COCOO}^- \xrightarrow{k_2} \text{E-LThDP}^- \xrightarrow{k_3} \text{E-HEThDP}^- \quad (8)$$

The time-resolved conversion of ThDP to HEThDP with the transient formation of LThDP (data not shown) at substrate saturation was fitted to a consecutive reaction mechanism (eq 8) showing that the covalent pyruvate binding at C2 of ThDP is clearly slower in the isolated E1 component as compared to the PDH complex. This process is composed of two phases with rate constants k_2 (E1) of 2 and 0.01 s^{-1} in comparison to the PDH complex (k_2 (complex) = 102 s^{-1}). The decarboxylation of LThDP proceeds with comparable rate constants (k_3 (E1) = 2 s^{-1}, k_3 (complex) = 6 s^{-1}). The ability to directly observe covalent intermediates and to time-resolve their interconversions on E1 in the complex or alone is the prerequisite for investigating the mechanism of catalytic steps and the principles of the regulation of this important enzyme at a molecular level.

In addition to the studies on pyruvate-converting enzymes, this NMR approach was applied to transketolase from *S.*

cerevisiae (TK, EC 2.2.1.1), which catalyzes the ketol transfer of a 2-carbon fragment between ketose phosphates (donor substrate) and aldose phosphates (acceptor substrate). The addition of the native donor substrates D-xylulose 5-P or D-fructose 6-P to TK leads to the transient formation of acid-stable, covalent ThDP intermediates (I1 and I2, respectively), both of which decompose to DHEThDP (Figure 4C). In the further reaction, DHEThDP is converted to ThDP (data not shown). The ^{1}H NMR signals of the sugar moieties of I1 and I2 interfere with the resonances of the donor sugar substrates and cannot be assigned unequivocally. However, the chemical reaction suggests that I1 and I2 must be the 2-[2-(1,2,3,4,5-pentahydroxy)-pentyl]-ThDP and 2-[2-(1,2,3,4,5,6-hexahydroxy)-hexyl]-ThDP derivatives, respectively. In accordance with recent X-ray crystallography data (*32*), the conversion of the artificial donor substrate β-hydroxy-pyruvate leads also to the accumulation of DHEThDP in the course of TK catalysis (Figure 4C). Our data clearly demonstrate that the ^{1}H NMR-based intermediate analysis can be applied successfully not only to pyruvate-converting enzymes but also to a prominent enzyme in sugar metabolism.

CONCLUSION

The possibility of freezing an enzyme in action and analyzing the distribution of all intermediates directly is rare in enzymology. One of the few other described cases is wild-type dTDP-glucose 4,6-dehydratase, a NAD-dependent enzyme (*33*). In this enzyme, the formation of intermediates under single turnover conditions was observed by mass spectrometry after rapid mix-quench. The data presented here demonstrate the feasibility of a chemical quench/NMR technique for the determination of the quantitative distribution of intermediates in an enzymic reaction not only under single turnover conditions but also at steady-state. From the steady-state intermediate distribution, the microscopic rate constants can be determined independently of their magnitude and of instrumental limitations (dead time). Therefore, rate constants are measurable that may range up to thousands per second. This new method described here, in combination with site-directed mutagenesis, enables a functional assignment of side chains in enzymic mechanisms. The analysis of the reaction mechanism of PDC confirmed the proposed least motion, maximum overlap mechanism of decarboxylation, and unraveled the coaction of two independent proton relay systems in the course of proton-transfer processes.

ACKNOWLEDGMENT

We gratefully acknowledge helpful discussions with P. Frey, D. Kern, and S. Ghisla. We thank J. Brauer, C. Simm, and B. Seliger for excellent technical assistance. We thank M. Vyazmensky and A. Bar-Ilan for preparation of the plasmid used to express *Ec*AHAS II and A. Chang, C.-Y. Huang, and Y.-G. Wu for providing the various *Zm*PDC mutant plasmids.

REFERENCES

1. Schellenberger, A. (1998) *Biochim. Biophys. Acta 1385*, 177−186.
2. Schowen, R. L. (1998) in *Comprehensive Biological Catalysis* (Sinnot, M., Ed.) Vol. 2, pp 217−266, Academic Press, London.
3. Kern, D., Kern, G., Neef, H., Tittmann, K., Killenberg-Jabs, M., Wikner, C., Schneider, G., and Hübner, G. (1997) *Science 275*, 67−70.
4. Alvarez, F. J., Ermer, J., Hübner, G., Schellenberger, A., and Schowen, R. L. (1991) *J. Am. Chem. Soc. 113*, 8402−8409.
5. Sun, S., Duggleby, R. G., and Schowen, R. L. (1995) *J. Am. Chem. Soc. 117*, 7317−7322.
6. Sergienko, E. A., Wang, J., Polovnikova, L., Hasson, M. S., McLeish, M. J., Kenyon, G. L., and Jordan, F. (2000) *Biochemistry 39*, 13862−13869.
7. Huang, C.-Y., Chang, A. K., Nixon, P. F., and Duggleby, R. G. (2001) *Eur. J. Biochem. 268*, 3558−3565.
8. Sergienko, E. A., and Jordan, F. (2001) *Biochemistry 40*, 7382−7403.
9. Muller, Y. A., and Schulz, G. E. (1993) *Science 259*, 965−967.
10. Arjunan, P., Umland, T., Dyda, F., Swaminathan, S., Furey, W., Sax, M., Farrenkopf, B., Gao, Y., Zhang, D., and Jordan, F. (1996) *J. Mol. Biol. 256*, 590−600.
11. Dobritzsch, D., König, S., Schneider, G., and Lu, G. (1998) *J. Biol. Chem. 273*, 20196−20204.
12. Lindqvist, Y., Schneider, G., Ermler, U., and Sundstrom, M. (1992) *EMBO J. 11*, 2373−2379.
13. Pang, S. S., Duggleby, R. G., and Guddat, L. W. (2002) *J. Mol. Biol. 317*, 249−262.
14. Arjunan, P., Nemeria, N., Brunskill, A., Chandrasekhar, K., Sax, M., Yan, Y., Jordan, F. Guest, J. R., and Furey, W. (2002) *Biochemistry 41*, 5213−5221.
15. Kluger, R., and Smyth, T. (1981) *J. Am. Chem. Soc. 103*, 884−888.
16. Krampitz, L., Greull, G., Miller, C. S., Bicking, J. B., Skeggs, H. R., and Sprague, J. M. (1958) *J. Am. Chem. Soc. 80*, 5893−5894.
17. Holzer, H., and Beaucamp, K. (1959) *Angew. Chem. 24*, 776.
18. Gruys, K. J., Halkides, C. J., and Frey, P. A. (1987) *Biochemistry 26*, 7575−7585.
19. Sergienko, E. A., and Jordan, F. (2001) *Biochemistry 40*, 7369−7381.
20. Bar-Ilan, A., Balan, V., Tittmann, K., Golbik, R., Vyazmensky, M., Hübner, G., Barak, Z., and Chipman, D. (2001) *Biochemistry 40*, 11946−11954.
21. Tittmann, K., Golbik, R., Ghisla, S., and Hübner, G. (2000) *Biochemistry 39*, 10747−10754.
22. Korotchkina, L. G., and Patel, M. S. (2001) *J. Biol. Chem. 276*, 37223−37229.
23. Wikner, C., Meshalkina, L., Nilsson, U., Nikkola, M., Lindqvist, Y., Sundström, M., and Schneider, G. (1994) *J. Biol. Chem. 269*, 32144−32150.
24. Liu, M., Sergienko, E. A., Guo, F., Wang, J., Tittmann, K., Hübner, G., Furey, W., and Jordan, F. (2001) *Biochemistry 40*, 7355−7368.
25. Lobell, M., and Crout, D. H. G. (1996) *J. Am. Chem. Soc. 118*, 1867−1873.
26. Kluger, R. (1987) *Chem. Rev. 87*, 863−876.
27. Turano, A., Furey, W., Pletcher, J., Sax, M., Pike, D., and Kluger, R. (1982) *J. Am. Chem. Soc. 104*, 3089−3095.
28. Friedemann, R., and Breitkopf, C. (1996) *Intl. J. Quantum Chem. 57*, 943−948.
29. Wu, Y.-G., Chang, A. K., Nixon, P. F., Li, W., and Duggleby, R. G. (2000) *Eur. J. Biochem. 267*, 6493−6500.
30. Ciskanik, L. M., and Schloss, J. V. (1985) *Biochemistry 24*, 3357.
31. Chipman, D., Barak, Z., and Schloss, J. V. (1998) *Biochim. Biophys. Acta 1385*, 401−419.
32. Fiedler, E., Thorell, S., Sandalova, T., Golbik, R., König, S., and Schneider, G. (2002) *Proc. Natl. Acad. Sci. U.S.A. 99*, 591−595.
33. Gross, J. W., Hegeman, A. D., Vestling, M. M., and Frey, P. A. (2000) *Biochemistry 39*, 13633−13640.

BI034465O